Journal of Alloys and Compounds 509 (2011) 2414–2419

Contents lists available at ScienceDirect

Journal of Alloys and Compounds

journal homepage: www.elsevier.com/locate/jallcom

Effect of annealing on structural and optoelectronic properties of nanostructured ZnSe thin films

M. Ashraf[a], S.M.J. Akhtar[a], A.F. Khan[b], Z. Ali[a], A. Qayyum[c,*]

[a] Optics Laboratories, P.O. Box 1021, Islamabad, Pakistan
[b] Pakistan Institute of Engineering and Applied Sciences (PIEAS), Islamabad, Pakistan
[c] Physics Division, Pakistan Institute of Nuclear Science and Technology, P.O. Nilore, Islamabad, Pakistan

ARTICLE INFO

Article history:
Received 14 July 2010
Received in revised form 4 November 2010
Accepted 4 November 2010
Available online 13 November 2010

Keywords:
ZnSe thin films
Optical band gap
Annealing effect
Semiconductor
Refractive index

ABSTRACT

Thin films of ZnSe were deposited on soda lime glass substrates by thermal evaporation and annealed in vacuum at various temperatures in the range of 100–300 °C. Structural and optoelectronic properties of these films were investigated and compared with the available data. XRD studies revealed that as-deposited films were polycrystalline in nature with cubic structure. It was further observed that the grain size and crystallinity increased, whereas dislocations and strains decreased with the increase of annealing temperature. The optical energy band gap estimated from the transmittance data was in the range of 2.60–2.67 eV. The observed increase in band gap energy with annealing temperature may be due to the quantum confinement effects. Similarly, refractive index of the films was found to increase with the annealing temperature. The AFM images revealed that films were uniform and pinhole free. The RMS roughness of the films increased from 1.5 nm to 2.5 nm with the increase of annealing temperature. Resistivity of the films decreased linearly with the increase of temperature.

© 2010 Elsevier B.V. All rights reserved.

1. Introduction

Zinc selenide (ZnSe) has unique physical properties, such as wide optical energy band gap (~2.7 eV), high refractive index, low optical absorption in the visible and infrared spectral region. ZnSe films, therefore, have several potential applications in electro-optics devices [1,2], optical coatings, thin film transistors and heterojunction solar cells [3]. At present CdS is the most extensively used buffer layer material for solar cells. However, due to the toxic nature of CdS layers much attention has been focused on developing Cd-free buffer layers. One such substitute of CdS is ZnSe. ZnSe is not only environment friendly but have wider band gap as compared to CdS (~2.4 eV), consequently ZnSe buffer layer may transmit even higher energy photons to the absorber layer of the solar cell. There are reports in the literature that it is possible to fabricate ZnSe based solar cells with efficiency >11% [4,5].

Among the various techniques that have been used to prepare ZnSe thin films [6–8], thermal evaporation is relatively simple, low cost and provide high deposition rate. It is well known that the structural and optical properties of a thin film depend very much on the conditions in which the deposition has been carried out. However, the properties of as-deposited thin film could be tailored, to some extent, by thermal annealing. For annealing treatment, various annealing parameters such as temperature, duration, atmosphere and pressure could be varied. Previously, the influence of annealing parameters on the properties of ZnSe thin film have been investigated, for instance Bacaksiz et al. [9] showed that annealing temperature of 200–400 °C did not affect the predominant (1 1 1) crystallographic texture but affected the degree of preferred orientation of ZnSe thin film deposited at the substrate of −73 °C and 275 °C. Also there was no appreciable change in optical band gap with annealing temperature. The annealing process reduced the electrical resistivity of the film deposited at −73 °C, but opposite trend was observed for the film deposited at 275 °C. Kale and Lokhande [10] reported that thermal annealing transformed metastable cubic phase into stable polycrystalline hexagonal phase, slightly reduced the optical band gap and electrical resistivity of the ZnSe thin films prepared by chemical bath deposition method. Oh et al. [11] prepared low resistivity p-type ZnSe epilayer by annealing ZnSe film in N_2 environment.

In this work, ZnSe thin films were deposited on the soda lime glass substrates by thermal evaporation and annealed at various temperatures in vacuum for 1 h. The effects of thermal annealing on the structural, optical and electrical properties of the films have been investigated and discussed.

2. Experimental setup

High purity (99.99%) ZnSe material was used as a source material for the deposition of ZnSe films on soda lime glass substrates. The substrates were cleaned with detergent and washed in running water followed by cleaning with isopropyl alcohol (IPA) in an ultrasonic bath. The films were deposited by resistive heating technique, using a high vacuum coating unit (Edward 610A). The vacuum better than

* Corresponding author. Tel.: +92 51 2207241; fax: +92 51 2207374.
E-mail address: qayyum@pinstech.org.pk (A. Qayyum).

0925-8388/$ – see front matter © 2010 Elsevier B.V. All rights reserved.
doi:10.1016/j.jallcom.2010.11.032

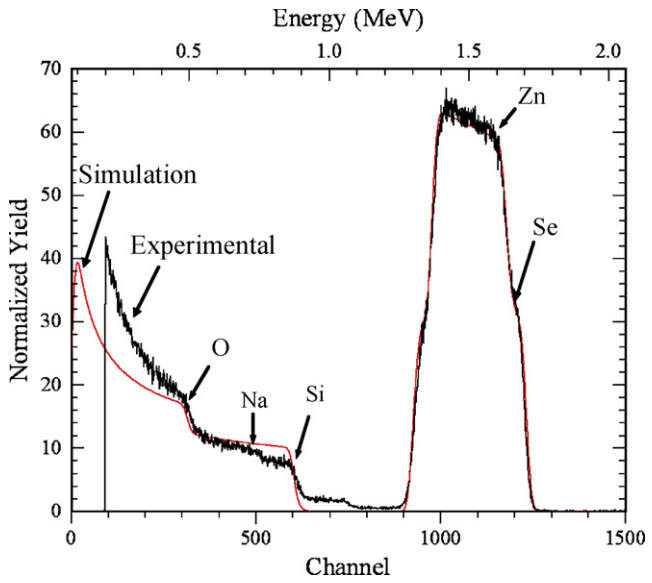

Fig. 1. Rutherford back scattering spectrum of ZnSe film annealed at 200 °C.

1×10^{-5} mbar was maintained in the chamber during deposition. The substrate was kept at room temperature (~25 °C) during deposition. The source to substrate distance was kept 35 cm and the substrate holder was rotated at 35 revolutions per minute. Film thickness and deposition rate were controlled by in situ quartz crystal monitor (FTM5). Average deposition rate and intended thickness of the films were 1.2 nm/s and 500 nm, respectively.

The films were annealed in vacuum (about 1×10^{-5} mbar) at various temperatures ranging from 100 to 300 °C for 1 h. Structure of these films was determined by X-ray diffraction (XRD) at room temperature. XRD measurements were performed using Bruker D8 discover diffractometer equipped with Cu K_α radiation in the scanning mode. Optical transmission of the films was recorded at room temperature in the wavelength range of 300–2500 nm using PerkinElmer Lambda 19 UV/vis/NIR Spectrophotometer and UV Win Lab software.

Band gape and refractive indices of these films were calculated by fitting the transmittance data. The surface morphology of the films was investigated by atomic force microscope (AFM) (Quesant Universal SPM, Ambios Technology, USA). The contact mode of operation was used to study the morphology of the film. An AFM tip of silicon nitride having radius of curvature ~10 nm was used. All images were taken in air ambient. The mean RMS roughness was taken at different sites of each film at atmospheric pressure and room temperature. The composition of the films was measured by Rutherford back scattering (RBS) technique. The 2.08 MeV doubly charged helium ions beam was used for the analysis. The RBS results were simulated by a computer code named RUMP. Electrical resistivity of the ZnSe films was measured using two-probe method.

3. Results and discussion

3.1. Composition and surface analysis

The deposited ZnSe thin films were uniform, pinhole free and well adherent with the substrate. Fig. 1 shows a typical RBS spectrum of ZnSe film annealed at 200 °C along with simulated spectrum. The RBS results revealed that films were nearly stoichiometric along with Si, Na and O elements from the substrate. Thickness of the films determined by RBS technique, quartz crystal and fitting the transmittance data were in good agreement. Fig. 2 depicts 3D AFM images of the films annealed at 100 and 300 °C. The photographs indicate that the films are smooth and continuous without any pinholes/cracks. AFM images also revealed that the grain size increases with the annealing temperature, which is also confirmed by XRD data (see below). RMS roughness of the films annealed at 100 and 300 °C was 1.5 nm and 2.5 nm, respectively, indicating that roughness increases with the increase of annealing temperature.

3.2. Structural properties

Fig. 3 shows XRD patterns of as-deposited and annealed ZnSe films. It is observed that all films are polycrystalline in nature having cubic crystal structure, preferred orientated along (1 1 1) together with other planes (2 2 0) and (3 1 1). Our results are in good agreement with the previous studies [12,13], which showed that ZnSe films grown by thermal evaporation have cubic structure. However, hexagonal wurtzite structure and cubic zinc blend structure, or some times a mixture of both phases have been observed for the ZnSe films deposited by various other techniques [14]. This shows that the structure of ZnSe films depends mostly on the deposition technique. Fig. 3 also shows that the intensity of (1 1 1) reflection increases with the annealing temperature. We attribute this increase of peak intensity to the enhancement of clusters, rearrangement of atoms and removal of residual stresses/defects formed during the film deposition [15]. Subbaiah et al. [14] reported similar increase of (1 1 1) reflection with the increase of substrate temperature up to 300 °C for ZnSe films deposited by close-spaced sublimation. The peaks due to (2 2 0) and (3 1 1) reflections became weak at higher annealing temperatures because of the improvement in crystallinity of the films. The average crystallite size, τ, was estimated using Scherrer formula [16]:

$$\tau = \frac{K\lambda}{\beta \cos\theta} \tag{1}$$

where K is the shape factor that was taken equal to 0.9, λ is the wavelength of X-ray source, β is the full width at half maximum (FWHM) of (1 1 1) peak and θ is the Bragg diffraction angle in degrees.

The lattice spacing, d, is calculated from the Bragg's formula:

$$d = \frac{\lambda}{2 \sin\theta} \tag{2}$$

The lattice parameter, a, for cubic ZnSe film was determined using the relation:

$$\frac{1}{d^2} = \frac{h^2 + k^2 + l^2}{a^2} \tag{3}$$

where h, k and l represent the lattice planes.

The dislocation density was determined using following the relation [17]:

$$\delta = \frac{15\beta \cos\theta}{4a\tau} \tag{4}$$

The strain ε values were evaluated by the following relation [18]:

$$\varepsilon = \frac{\beta \cos\theta}{4} \tag{5}$$

Structural parameters for the (1 1 1) peak such as lattice constant a, lattice spacing d, grain size τ, dislocation density δ, and strain ε are summarized in Table 1. Data shows that the lattice constant of the films deviates from the bulk which indicates that crystallites of films are under strained that may be due to the change in nature and concentration of the native defects [13]. The strain and dislocation density decreases, whereas grain size increases with the increase of annealing temperature, which indicates the improvement in crystallinity of the films.

3.3. Optical properties

The optical parameters of ZnSe thin films, thickness and the refractive index were calculated by fitting the transmission data to the following equation [19,20]:

$$T = \frac{Ax}{B - Cx\cos\phi + Dx^2} \tag{6}$$

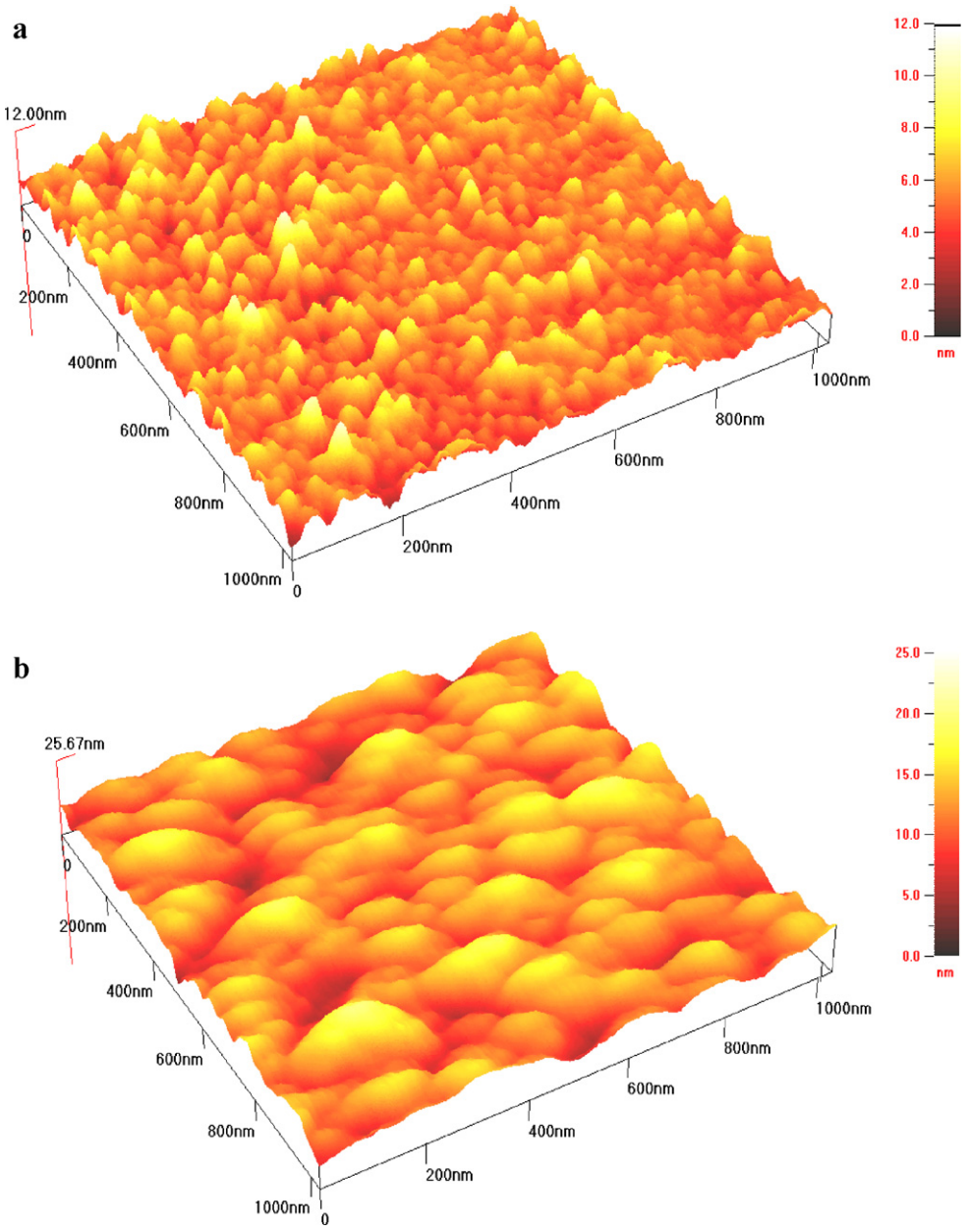

Fig. 2. Three dimensional AFM (1000 nm × 1000 nm) images showing the surface morphology of ZnSe films; annealed in vacuum for 1 h at (a) 100 °C and (b) 300 °C.

where T is the normal transmittance of the system consisting of a thin film on a transparent substrate surrounded by air, and taking into account all multiple reflections at the interface for the case of $k^2 \ll n^2$, which is true for this kind of semiconductor thin films [20–22]. The other variables are defined as $A = 16n^2s$, $B = (n+1)^3\ (n+s^2)$, $C = 2(n^2-1)(n^2-s^2)$, $D = (n-1)^3\ (n-s^2)$, $\phi = 4\pi nd/\lambda$, $x = \exp(-\alpha d)$, $k = \alpha\lambda/4\pi$. Here n and s are the refractive index of the film and glass substrate respectively, d is the thickness, α is the absorption coefficient and k is the extinction coefficient of the film. An empirical formula for n dependence of λ is given as [19,20]:

$$n = a + \frac{b}{\lambda^2} \tag{7}$$

where a and b are constants. The α dependence of λ can be approximated as

$$\alpha = c + \frac{f}{\lambda} + \frac{g}{\lambda^2} \tag{8}$$

Table 1
The structural parameters for (1 1 1) peak of ZnSe films annealed at various temperatures.

Annealing temperature (°C)	2θ (°)	a (Å)	d (Å)	Grain size τ (nm)	Strain × 10^{-3} ε (lin^{-2} m^{-4})	Dislocation density × 10^{15} δ (lin m^{-2})
25 (as deposited)	27.17	5.680	3.279	20.50	1.70	2.30
100	27.21	5.675	3.276	25.70	1.39	1.49
200	27.20	5.674	3.275	41.00	0.90	0.60
300	27.21	5.675	3.276	45.20	0.80	0.49

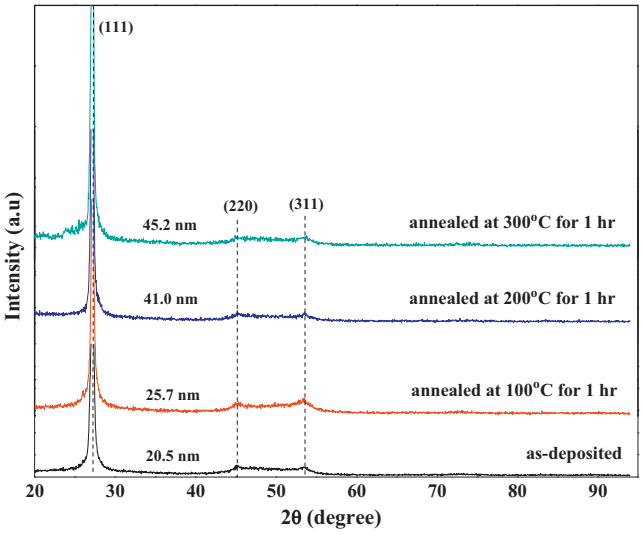

Fig. 3. X-ray diffraction patterns of as-deposited and annealed ZnSe thin films.

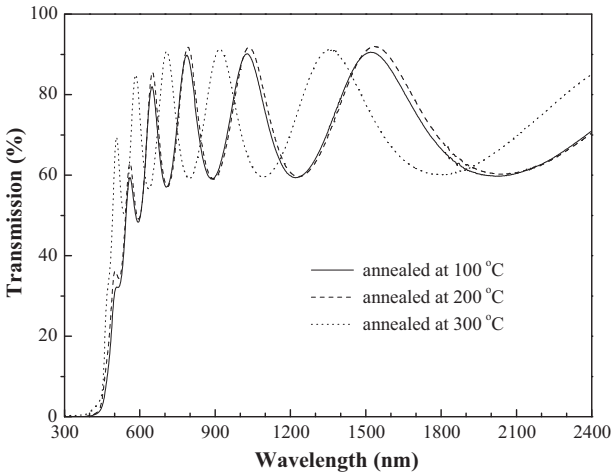

Fig. 5. Optical transmission of ZnSe films as a function of wavelength.

where c, f and g are constants. Fig. 4 shows the resulting fit of Eq. (6) to the experimental data. It is clear that it provides a good fit in transparent as well as in medium absorption region. By using the values of n and d, which were determined from the fitted curve, α was calculated in the high absorption region. In this case the exact solution of Eq. (6) for x is

$$x = \frac{[C\cos(\phi) + A/T] - [(C\cos(\phi) + A/T)^2 - 4BD]^{1/2}}{2D} \quad (9)$$

$$\alpha = -\frac{1}{d}\ln(x)$$

where all the parameters are defined earlier. Fig. 5 shows transmission of the films annealed at various temperatures as a function of wavelength. The interference peaks present in each spectrum confirm that the films are uniform. The sudden fall of transmission below 500 nm is most probably due to the absorption edge. The films annealed at 100 and 200 °C show less transmittance at shorter wavelengths, whereas film annealed at 300 °C revealed higher transmittance. The variation in absorption edge most probably due to the improvement in structural order, removal of residual stresses and quantum confinement effects [21–23]. The films showed blue shift with the increase of annealing temperature, which indicates that absorption edge shifting towards bulk ZnSe. The blue shift may be attributed with structural changes in the films such as growth of nanocrystallites into larger crystallites.

The direct energy band gap, E_g, was determined using the well-known relation $\alpha h\nu = (h\nu - E_g)^{1/2}$, where $h\nu$ is the photon energy. E_g of the ZnSe films annealed at various temperature were estimated by extrapolating the linear portion of $(\alpha h\nu)^2$ vs. $(h\nu)$ curves to $(\alpha h\nu)^2 = 0$ as shown in Fig. 6. The energy band gap of the films annealed at various temperatures is plotted in Fig. 7. The band gap at annealing temperature 300 °C was found to be 2.67 eV, which is very close to that of bulk ZnSe (2.70 eV) [24]. The increase in energy band gap from 2.60 to 2.67 eV may be related with the existence of high-density levels within the band gap [25] and the structural changes causing quantum confinement effects in the ZnSe films with annealing temperature [21–23]. The calculated values of band gap are in good agreement with that of the films deposited by vacuum evaporation (2.63–2.64 eV) [9], screen-printing (2.66 eV) [26] and two-source evaporation (2.68 eV) [27] methods. But the band gap values reported in this study are higher than that of the films deposited by closed spaced sublimation (2.57–2.61 eV) technique [14].

The refractive index of ZnSe films annealed at 100, 200 and 300 °C is plotted as a function of wavelength in Fig. 8. The refractive indices of all films are tabulated in Table 2. The reported values of refractive indices are in good agreement with films deposited by

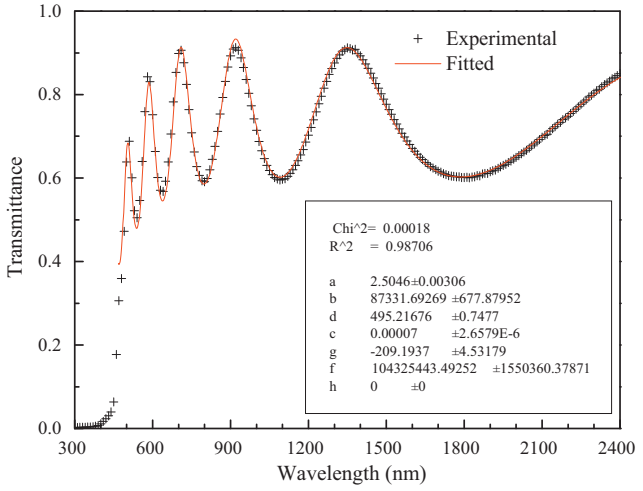

Fig. 4. Optical transmittance along with fitted spectrum of ZnSe film annealed at 300 °C.

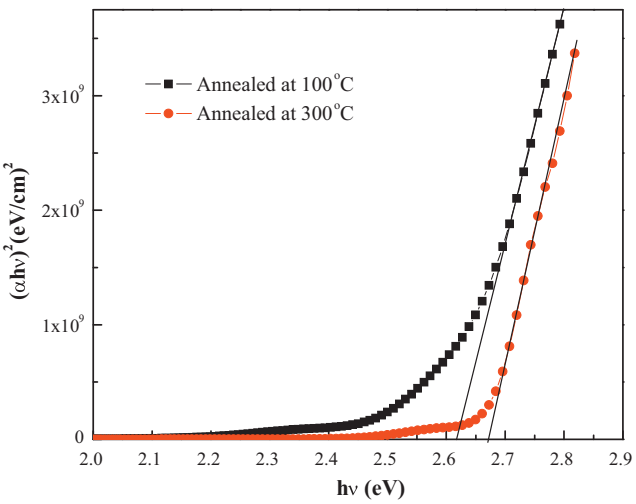

Fig. 6. Plot of $(\alpha h\nu)^2$ vs. photon energy $(h\nu)$ of ZnSe films.

Table 2
Optical parameters of ZnSe films annealed at various temperatures.

Annealing temperature (°C)	Refractive index, $n = a + b/\lambda^2$		Band gap E_g (eV)	Thickness of films determined by fitting (nm)
	a	b (nm)^2		
25 (as deposited)	2.4801	8.5618×10^4	2.60	540
100	2.4883	8.5812×10^4	2.62	530
200	2.49363	8.8249×10^4	2.63	520
300	2.5046	8.7331×10^4	2.67	495

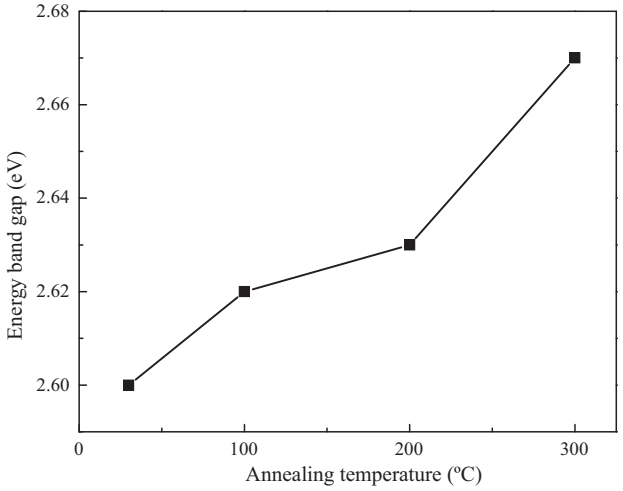

Fig. 7. Energy band gap of ZnSe films as a function of annealing temperature.

hot wall evaporation ($n \sim 2.75$ at 550 nm) [28], but higher than the values reported for the film deposited by closed spaced sublimation ($n \sim 2.54$ at 550 nm) [14]. Our results indicate that refractive index increases with the increase of annealing temperature that may due to the improvement in crystalline structure, increase of grain size and reduction of dislocation density (Table 1).

3.4. Electrical properties

The electrical resistivity of ZnSe thin films was measured in the temperature range of 300–550 K. For this study samples were cut into dimensions of 10 mm × 10 mm, gold coating was used to make the contact and silver paste for wire connections. The resistivity of semiconductor at any temperature T is given by the Arrhenius relation.

$$\rho = \rho_0 \exp\left(\frac{Ea}{kT}\right) \quad (10)$$

where ρ_0 is constant, k is Boltzmann's constant and Ea is activation energy. The variation of resistivity with absolute temperature is shown in Fig. 9. Linear behavior of the graph indicates that the film conductivity is in good agreement with the Arrhenius relation. The activation energy of as deposited film calculated from slope of the graph is ~0.45 eV. The decrease in resistivity with increase of temperature indicates the semi-conducting behavior of ZnSe films. The reduction of resistivity with the increase of temperature may be due to the thermal excitation of carriers from the grain boundaries to the region of grains [29]. The low temperature conductivity can be explained by hopping of carriers between the localized states (Efors–Shkloskii conduction mechanism), whereas at high temperatures Mott's hopping may be responsible for the higher conductivity [30].

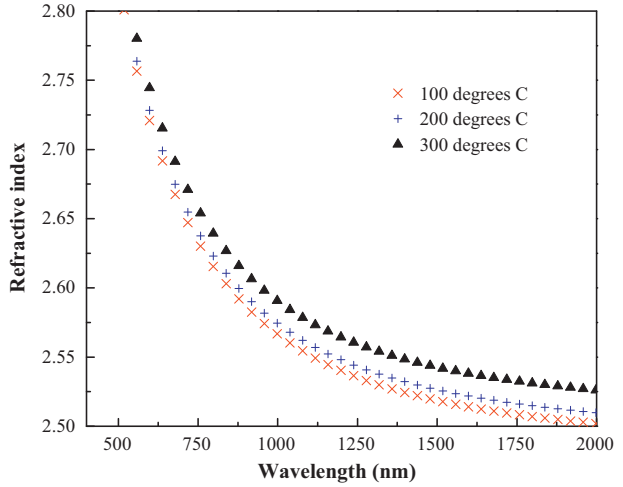

Fig. 8. Refractive index of ZnSe films as a function of wavelength.

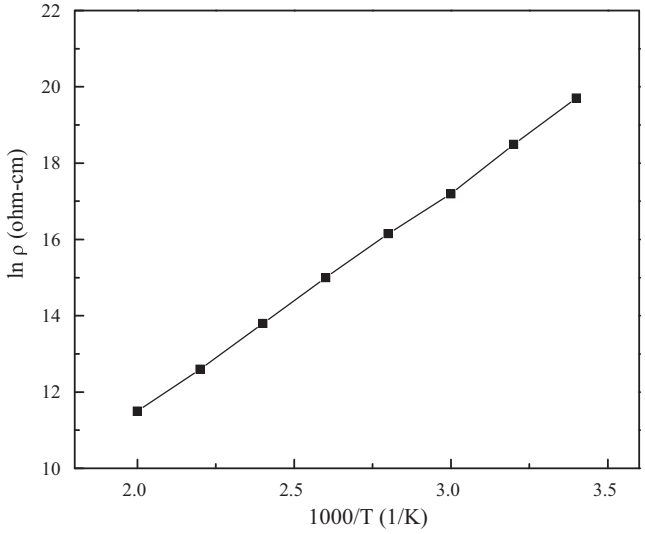

Fig. 9. Temperature dependence of resistivity of as deposited ZnSe film.

4. Conclusions

The ZnSe thin films have been deposited on glass substrates by vacuum evaporation and annealed in vacuum at various temperatures. Deposited films were uniform and pinhole free. All the films were nearly stoichiometric and have a cubic structure with preferred orientation along (1 1 1) plane. The crystalline quality of the film found to increase with the increase of annealing temperature. Optical studies revealed that the energy band-gap and refractive index increases with the increase of annealing temperature. Electric analysis showed linear increase in conductivity of the film with the annealing temperature. The results reported in this paper are useful for the designing of optoelectronic devices, optical coating for infrared applications and buffer layer for solar cells.

References

[1] B. Güzeldir, M. Sağlam, A. Ateş, J. Alloys Compd. 506 (2010) 388–394.
[2] A. Othonos, E. Lioudakis, D. Tsokkou, U. Philipose, H.E. Ruda, J. Alloys Compd. 483 (2009) 600–603.
[3] P.P. Hankare, P.A. Chate, P.A. Chavan, D.J. Sathe, J. Alloys Compd. 461 (2008) 623–627.
[4] A. Ennaoui, S. Siebentritt, M.Ch. Lux-Steiner, W. Riedl, F. Karg, Sol. Energy Mater. Sol. C 67 (2001) 31–40.
[5] W. Eisele, A. Ennaoui, P. Schubert-Bischoff, M. Giersig, C. Pettenkofer, J. Krauser, M. Lux-Steiner, S. Zweigart, F. Karg, Sol. Energy Mater. Sol. C 75 (2003) 17–26.
[6] A. Manzoli, K.I.B. Eguiluz, G.R. Salazar-Banda, S.A.S. Machado, Mater. Chem. Phys. 121 (2010) 58–62.
[7] A.M.E. Raj, S.M. Delphine, C. Sanjeeviraja, M. Jayachandran, Physica B 405 (2010) 2485–3249.
[8] Y.G. Gudage, N.G. Deshpande, A.A. Sagade, R. Sharma, J. Alloys Compd. 488 (2009) 157–162.
[9] E. Bacaksiz, S. Aksu, I. Polat, S. Yılmaz, M. Altunba, J. Alloys Compd. 487 (2009) 280–285.
[10] R.B. Kale, C.D. Lokhande, Appl. Surf. Sci. 252 (2005) 929–938.
[11] C.B. Oh, J.F. Wang, M. Isshiki, Curr. Appl. Phys. 4 (2004) 630–632.
[12] S. Venkatachalam, D. Soundarajan, P. Peranatham, D. Mangalaraj, S.K. Narayandass, S. Velumani, P.S. Retchkiman, Mater. Charact. 58 (2007) 715–720.
[13] S. Venkatachalam, D. Mangalaraj, S.K. Narayandass, K. Kim, J. Yi, Physica B 358 (2005) 27–35.
[14] Y.P. Venkata Subbaiah, P. Prathap, M. Devika, K.T. Ramakrishna Reddy, Physica B 365 (2005) 240–246.
[15] A.J. Alam, D.C. Cameron, Thin Solid Films 377–378 (2000) 455–459.
[16] B. Cullity, Elements of X-ray Diffraction, Addison-Wesley Company Inc., London, 1978, 99 pp.
[17] C.K. De, N. Mishra, Indian J. Phys. 71 (1997) 530.
[18] S. Venkatachalam, R.T. Rajendra Kumar, D. Mangalaraj, S.K. Narayandass, K. Kim, J. Yi, Solid State Electron. 48 (2004) 2219–2223.
[19] R. Swanepoel, J. Phys. E: Sci. Instrum. 16 (1983) 1214–1222.
[20] R. Swanepoel, J. Vac. Sci. Technol., J. Phys. E: Sci. Instrum. 17 (1984) 896–903.
[21] K. Prabhakar, Sa.K. Narayandass, D. Mangalaraj, J. Alloys Compd. 364 (2004) 23–28.
[22] G.L. Tan, J.H. Du, Q.J. Zhang, J. Alloys Compd. 468 (2009) 421–431.
[23] S. Thangavel, S. Ganesan, S. Chandramohan, P. Sudhagar, Y.S. Kang, C.-H. Hong, J. Alloys Compd. 495 (2010) 234–237.
[24] N.J.S. Kissinger, N. Velmurugan, K. Perumal, J. Korean Phys. Soc. 55 (2009) 1577–1581.
[25] L.Y. Sun, L.K. Kazamerski, A.H. Clark, P.J. Ireland, D.W. Morton, J. Vac. Sci. Technol. 15 (1978) 265.
[26] V. Kumar, K.L.A. Khan, G. Singh, T.P. Sharma, M. Hussain, Appl. Surf. Sci. 253 (2007) 3543–3546.
[27] Z. Ali, A.K.S. Aqili, A. Maqsood, S.M.J. Akhtar, Vacuum 80 (2005) 302–309.
[28] R. Pal, B. Maiti, S. Chaudhuri, A.K. Pal, Vacuum 46 (1996) 1255–1260.
[29] H.K. Sadekar, N.G. Deshpande, Y.G. Gudage, A. Ghosh, S.D. Chavhan, S.R. Gosavi, R. Sharma, J. Alloys Compd. 453 (2008) 519–524.
[30] A. Ganguly, S. Chaudhuri, A.K. Pal, J. Phys. D: Appl. Phys. 34 (2001) 506–513.